

DETECTING STRUCTURAL BRAIN CONNECTIVITY DIFFERENCES IN DEMENTIA THROUGH A CONDUCTANCE MODEL

Aina Frau-Pascual¹, Jean Augustinack¹, Divya Varadarajan¹,
Anastasia Yendiki¹, Bruce Fischl^{1,2}, and Iman Aganj^{1,2}

(1) A. A. Martinos Center for Biomedical Imaging, Massachusetts General Hospital, Harvard Medical School, Boston, MA, USA;

(2) Computer Science and Artificial Intelligence Laboratory, Massachusetts Institute of Technology, Cambridge, MA, USA

ABSTRACT

Structural brain connectivity has been shown to be sensitive to the changes that the brain undergoes during Alzheimer’s disease (AD) progression. In this work, we use our recently proposed structural connectivity quantification measure derived from diffusion MRI, which accounts for all possible neural pathways (direct and indirect) to quantify brain connectivity. We analyze data from the ADNI-2 and OASIS-3 datasets to derive relevant information for the study of the changes that the brain undergoes in AD.

Index Terms— connectivity, conductance, diffusion MRI, Alzheimer’s disease, dementia

1. INTRODUCTION

Brain structural connectivity can be measured by diffusion-weighted MRI (dMRI) and reflects the physical connectivity through white-matter axon bundles between different regions of interest (ROI). Differences in brain connectivity patterns between healthy and diseased populations are potential indicators of changes in the brain “wiring” due to disease processes. In particular, Alzheimer’s disease (AD) has been found to impact structural connectivity [1, 2]. Accurately modeling structural connectivity may therefore reveal the effects of AD progression in white-matter degeneration.

We have previously introduced a conductance method for inferring structural brain connectivity from dMRI [3], which accounts for all possible white-matter pathways, and is solved globally. This method was shown to be more strongly correlated with resting-state functional connectivity and more sensitive to AD-related white-matter degeneration than standard streamline tractography methods.

In this work, we extend our analysis to focus on the impact that this measure could have in the study of AD dementia. For this, we compare structural connectivity with cognitive and volumetric measures, and we also analyze additional datasets that provide examples of the power of our technique.

2. CONDUCTANCE MODEL

In our previous work [3]¹, we extended the heat equation method proposed by O’Donnell et al [4] with a combination of differential circuit laws. We assigned to each image voxel a local anisotropic conductivity value D , which is the diffusion tensor computed from dMRI [5, 6]. By solving the partial differential equation (PDE) [7],

$$-\nabla \cdot (D\nabla\phi_{i,j}) = \gamma_{i,j}, \quad (1)$$

for a certain current configuration $\gamma_{i,j}$ between a pair of source (i) and sink (j) voxels (see below), we find the potential map $\phi_{i,j}$ for that specific configuration. ∇ and $\nabla \cdot$ are the gradient and the divergence operators, respectively.

We solve the PDE for a 1-ampere current (without loss of generality) between a pair of voxels i and j : $\gamma_{i,j} = \delta_i - \delta_j$, where $\delta_k(x) := \delta(x - x_k)$, with x_k the position of voxel k and $\delta(\cdot)$ the Dirac delta. To compute ROI-wise conductance, we distribute the currents among the sets of voxels I and J (the two ROIs) as: $\gamma_{I,J} = \frac{1}{|I|} \sum_{i \in I} \delta_i - \frac{1}{|J|} \sum_{j \in J} \delta_j$.

The conductance between two points can then be computed with Ohm’s law as the ratio of the current to the potential difference. In our case, we set a 1-ampere current between two voxels (or ROIs) i and j , and the potential difference is $\phi_{i,j}(x_i) - \phi_{i,j}(x_j)$. The conductance is therefore computed, voxel-wise, as:

$$C_{i,j} = \frac{1}{\phi_{i,j}(x_i) - \phi_{i,j}(x_j)}. \quad (2)$$

For ROI-wise connectivity, we have:

$$C_{I,J} = \frac{1}{\frac{1}{|I|} \sum_{i \in I} \phi_{I,J}(x_i) - \frac{1}{|J|} \sum_{j \in J} \phi_{I,J}(x_j)}. \quad (3)$$

Using the superposition principle, we can use a sink point s as reference and reduce the number of computations from $O(N^2)$ to $O(N)$:

$$\begin{aligned} -\nabla \cdot (D\nabla(\phi_{i,s} - \phi_{j,s})) &= -\nabla \cdot (D\nabla\phi_{i,s}) + \nabla \cdot (D\nabla\phi_{j,s}) \\ &= (\delta_i - \delta_s) - (\delta_j - \delta_s) = \delta_i - \delta_j = -\nabla \cdot (D\nabla\phi_{i,j}). \end{aligned} \quad (4)$$

¹Our codes are publicly available at:
www.nitrc.org/projects/conductance

High conductance (i.e. low resistance) between two points represents a high degree of connectivity in our model. Note that the ROIs are all at least weakly connected, and that these maps could be thresholded.

3. ANALYSIS OF AD POPULATION

In this work, we evaluate how our conductance method can help in discriminating different stages of AD. For this, we use two publicly available datasets: the second phase of Alzheimer’s Disease Neuroimaging Initiative (ADNI-2) [8, 9], and the third phase of the Open Access Series of Imaging Studies (OASIS-3) [10], which is the longitudinal neuroimaging, clinical, and cognitive dataset for normal aging and AD. These two datasets allow us to compare structural brain connectivity in different stages of the disease and correlate neuroimaging data to clinical cognitive scores.

3.1. MR data processing

The common pipeline for brain connectivity computation is: segmentation of brain ROIs, quantification of brain connections from diffusion MRI, and aggregation of connectivity values in a matrix. The constructed brain connectivity matrix will describe how strongly different regions are connected to each other according to the diffusion MRI acquisition of white matter connections. We processed the MRI data similarly for both datasets.

3.1.1. Structural MR processing:

We performed tissue segmentation and parcellation of the cortex into ROIs using FreeSurfer² [11]. The parcellation used in this work is the Desikan-Killiany atlas [12].

3.1.2. Diffusion MRI processing:

Diffusion preprocessing was performed using the FSL software³ [13] and included BET for brain extraction and EDDY for eddy current and subject motion correction. From the preprocessed dMRI images, we reconstructed the diffusion tensors using the Diffusion Tensor Imaging (DTI) [5] reconstruction module of DSI Studio⁴, which we then used as input to our conductance approach. To compare with standard approaches, we also ran DSI Studio streamline tractography (ST) [14] using DTI, for direct comparison with our approach, and using generalized q-sampling imaging (GQI) [15], which, as opposed to DTI, can model multiple axon populations per voxel. We generated 10000 fiber tracts and used the default values for the rest of the parameters.

²FreeSurfer, <https://surfer.nmr.mgh.harvard.edu>

³FSL, <https://fsl.fmrib.ox.ac.uk/fsl/fslwiki>

⁴DSI Studio, <http://dsi-studio.labsolver.org>

3.1.3. Brain connectivity matrix generation:

For comparison with our conductance model, we also computed connectivity matrices using DSI Studio, considering the connectivity measure to be the tract count normalized by the median length, including tracts *passing* through the ROI. With our conductance equation model, we are proposing a new way of modeling and quantifying diffusion data. As we mentioned in the previous section, we split the 1-ampere current across voxels and solve the PDE once per ROI to find a conductance measure between each pair of ROIs through superposition.

3.2. Data description

We considered two datasets (see Figure 1) that include subjects across the AD dementia spectrum. In ADNI-2, we included 213 subjects, where 78 subjects were cognitively normal (CN), 90 subjects had mild cognitive impairment (MCI), a mid stage of the disease, and 47 subjects were diagnosed with AD dementia. In OASIS-3, we considered 272 subjects (its largest subset of subjects sharing identical scan description), where 187 subjects were cognitively normal, 38 subjects had AD dementia, and 47 had other types of dementia (e.g. vascular dementia, or AD dementia with depression or additional symptoms).

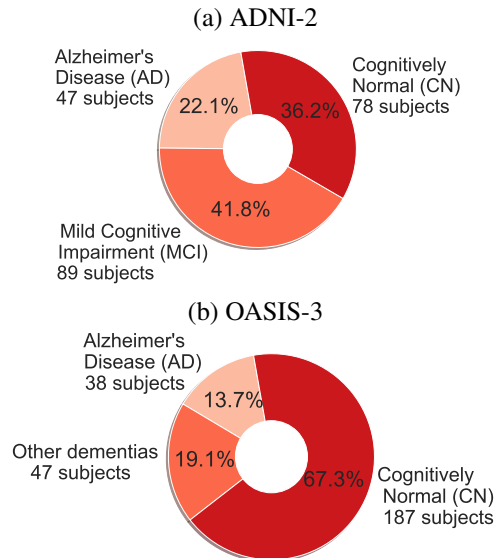


Fig. 1. Demographics of the two datasets used here.

Other clinical data from these populations were also available: age, diagnosis, cerebral cortical and subcortical volumes, β -Amyloid (a marker of AD) status, whether they have the APOE gene alleles that are related to AD, and cognitive scores such as the Clinical Dementia Rating (CDR) scale [16] and the Mini-Mental State Examination score [17]. CDR measures from 0 to 2 the cognitive capabilities of each subject, with 0 being cognitively normal and a higher number reflecting higher cognitive impairment. MMSE rates cognitive

capabilities from 0 to 30, with 30 being cognitively normal and a lower value reflecting higher cognitive impairment.

4. BRAIN CONNECTIVITY RESULTS

We have previously shown [3] that the conductance measure outperforms ST-derived connectivity at classifying disease stages in ADNI-2. Figure 2 shows the disease stage random-forest classification accuracy of this method with respect to streamline tractography and compared to cortical thickness and subcortical volume measures. When comparing the conductance results to cortical thickness and subcortical volume measures, which are the state of the art in MR-derived markers, the performance was similar. We tried combining these two measures and the results did not improve, which suggests that our measure of conductance most likely has overlap with volumetric measures.

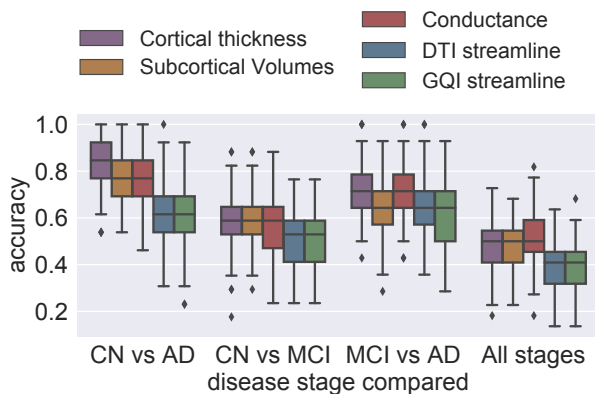


Fig. 2. Results extending [3]: The conductance method better classifies across disease stages, when looking at different AD-disease stages in ADNI-2 dataset.

With ADNI-2, we also tried classifying AD vs CN disease stages among only the β -Amyloid positive subjects, with a mean of $68\% \pm 20\%$ accuracy. Performance was the same for the conductance method, DTI ST and GQI ST.

In Figure 3, we attempted to predict CDR and MMSE cognitive scores by using simple linear regression. We achieved significant p -values in the case of ADNI-2 (Figure 3(a)), but not in OASIS-3 (Figure 3(b)). The prediction values were similar to using volume values and better than using ST-derived connectivity measures.

We further explored the OASIS-3 dataset (Figure 4) and found the mean of the conductance matrix to be significantly positively correlated with the MMSE score, cortical volumes, and subcortical volumes, and significantly negatively correlated with CDR and age. The correlations followed the same trend for ADNI-2, however much more significantly: $p = 0.00003$ for CDR, $p = 0.0004$ for MMSE, $p = 0.0000001$ for age, and $p = 0.000002$ and $p = 0.003$ for cortical and subcortical volumes respectively.

From the distribution of mean connectivity for the CN and AD dementia groups in Figure 5, we can see that the two distributions are overlapped but the means are separated ($t = 4.06, p = 0.00008$). When we plot according to the CDR scale, we see overlapped distributions again, with separated means: $t = 4.04, p = 0.00007$ between CDR= 0 and CDR= 0.5, $t = 2.31, p = 0.00007$ between CDR= 0.5 and CDR ≥ 1 , and $t = 5.1, p = 0.000007$ between CDR= 0 and CDR ≥ 1 . However, classification results were not as good as expected, probably due to unbalanced cohort size.

5. CONCLUSION

We have shown the applicability of our conductance method to detect brain changes correlated with AD. This method is sensitive to AD-related changes in both the diffusional and the geometric properties of the brain white matter. For instance, given that the method takes into account distances, changes in subcortical volumes and cortical thickness would also affect this measure of connectivity.

With the conductance method, we have shown better classification performance than streamline tractography in disease staging, and better prediction of cognitive scores and age with ADNI-2 data when using a simple linear regression. In OASIS-3, we see a correlation of the mean of conductance with cognitive and volume measures. However, classification of disease stages was not satisfactory for OASIS-3, probably due to the very unbalanced sample size (many fewer cases of AD than CN). Future work will be dedicated to the analysis of more datasets.

6. ACKNOWLEDGEMENTS

Support for this research was provided by the Bright-Focus Foundation (A2016172S). Additional support was provided by the National Institutes of Health (NIH), specifically the BRAIN Initiative Cell Census Network (U01MH117023), the National Institute of Diabetes and Digestive and Kidney Diseases (K01DK101631, R21DK108277), the National Institute for Biomedical Imaging and Bioengineering (P41EB015896, R01EB006758, R21EB018907, R01EB019956), the National Institute on Aging (AG022381, 5R01AG008122-22, R01AG016495-11, R01AG016495, 1R56AG064027), the National Center for Alternative Medicine (RC1AT005728-01), the National Institute for Neurological Disorders and Stroke (R01NS052585, R21NS072652, R01NS070963, R01NS083534, U01NS086625, R01NS105820), and the NIH Blueprint for Neuroscience Research (U01MH093765), part of the multi-institutional Human Connectome Project. Computational resources were provided through NIH Shared Instrumentation Grants (S10RR023401, S10RR019307, S10RR023043, S10RR028832). B. Fischl has a financial interest in CorticoMetrics, a company whose medical pursuits

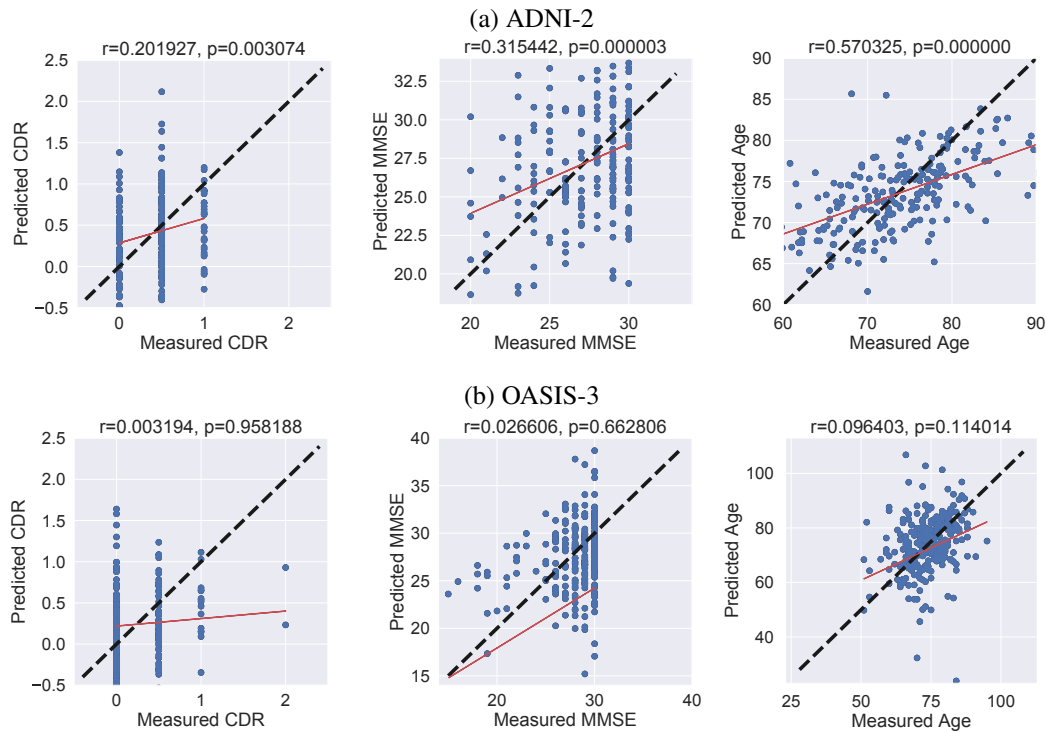


Fig. 3. Prediction of CDR, MMSE and age, from conductance matrices.

focus on brain imaging and measurement technologies. B. Fischl's interests were reviewed and are managed by MGH and Partners HealthCare in accordance with their conflict of interest policies.

References

- [1] S. E. Rose, F. Chen, J. B. Chalk, F. O. Zelaya, W. E. Strugnell, M. Benson, J. Semple, and D. M. Doddrell, "Loss of connectivity in Alzheimer's disease: an evaluation of white matter tract integrity with colour coded MR diffusion tensor imaging," *Journal of Neurology, Neurosurgery & Psychiatry*, vol. 69, no. 4, pp. 528–530, 2000.
- [2] G. Prasad, S. H. Joshi, T. M. Nir, A. W. Toga, P. M. Thompson, A. D. N. I. (ADNI *et al.*), "Brain connectivity and novel network measures for Alzheimer's disease classification," *Neurobiology of aging*, vol. 36, pp. S121–S131, 2015.
- [3] A. Frau-Pascual, M. Fogarty, B. Fischl, A. Yendiki, and I. Aganj, "Quantification of structural brain connectivity via a conductance model," *Neuroimage*, vol. 189, pp. 485–496, 2019.
- [4] L. O'Donnell, S. Haker, and C.-F. Westin, "New approaches to estimation of white matter connectivity in diffusion tensor MRI: Elliptic PDEs and geodesics in a tensor-warped space," in *International Conference on Medical Image Computing and Computer-Assisted Intervention*. Springer, 2002, pp. 459–466.
- [5] P. J. Basser, J. Mattiello, and D. LeBihan, "MR diffusion tensor spectroscopy and imaging," *Biophysical journal*, vol. 66, no. 1, pp. 259–267, 1994.
- [6] D. S. Tuch, V. J. Wedeen, A. M. Dale, J. S. George, and J. W. Belliveau, "Conductivity tensor mapping of the human brain using diffusion tensor MRI," *Proceedings of the National Academy of Sciences*, vol. 98, no. 20, pp. 11 697–11 701, 2001.
- [7] H. A. Haus and J. R. Melcher, *Electromagnetic fields and energy*. Prentice Hall, 1989.
- [8] C. R. Jack, M. A. Bernstein, N. C. Fox, P. Thompson, G. Alexander, D. Harvey, B. Borowski, P. J. Britson, J. L. Whitwell, C. Ward *et al.*, "The Alzheimer's disease neuroimaging initiative (ADNI): MRI methods," *Journal of magnetic resonance imaging*, vol. 27, no. 4, pp. 685–691, 2008.
- [9] L. A. Beckett, M. C. Donohue, C. Wang, P. Aisen, D. J. Harvey, N. Saito, A. D. N. Initiative *et al.*, "The Alzheimer's Disease Neuroimaging Initiative phase 2: Increasing the length, breadth, and depth of our understanding," *Alzheimer's & Dementia*, vol. 11, no. 7, pp. 823–831, 2015.

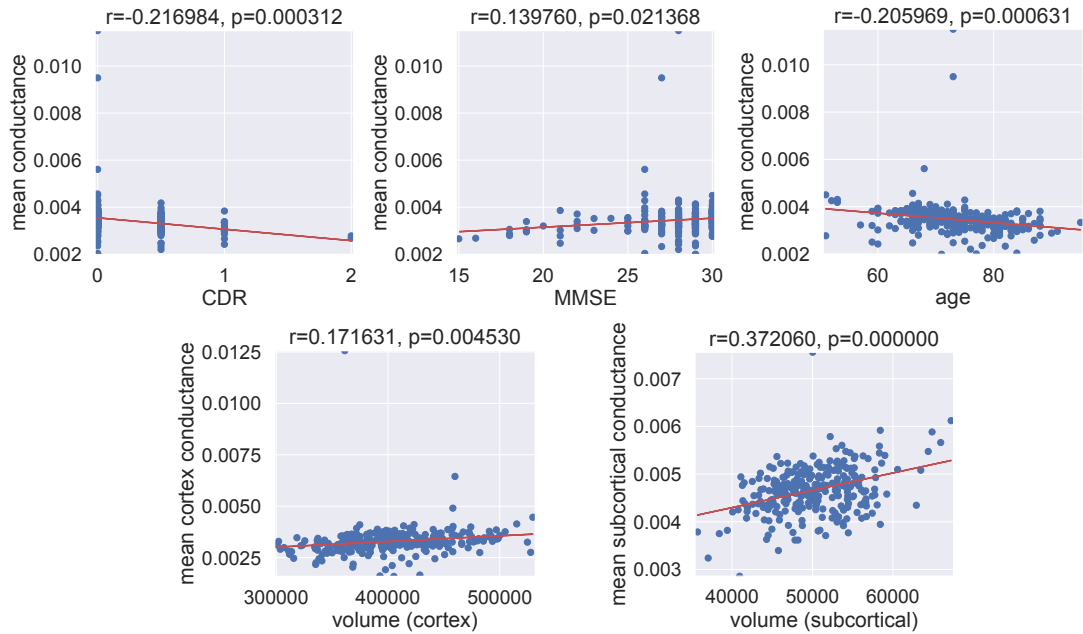


Fig. 4. Correlation of mean conductance with CDR and MMSE scores, with cortical and subcortical volumes, and with age.

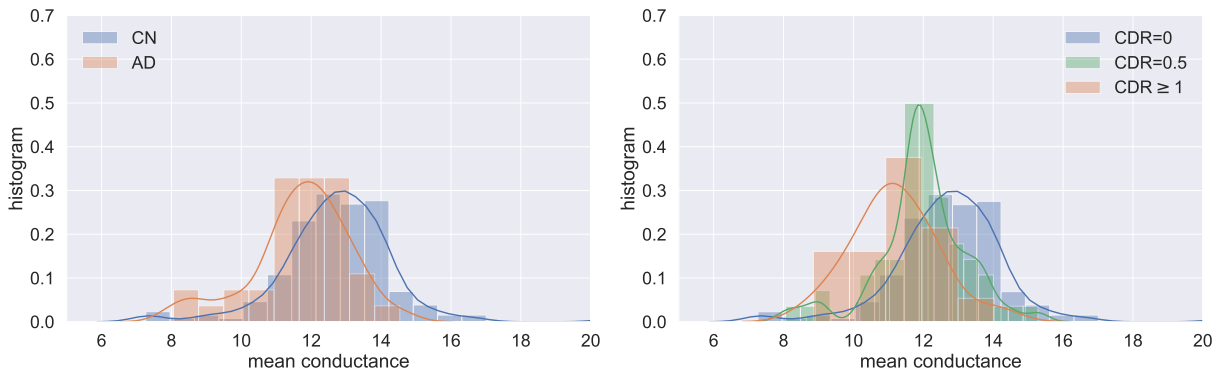


Fig. 5. Distribution of mean conductance across disease stage and CDR scales in OASIS-3.

- [10] A. F. Fotenos, A. Snyder, L. Girton, J. Morris, and R. Buckner, "Normative estimates of cross-sectional and longitudinal brain volume decline in aging and ad," *Neurology*, vol. 64, no. 6, pp. 1032–1039, 2005.
- [11] B. Fischl, "FreeSurfer," *Neuroimage*, vol. 62, no. 2, pp. 774–781, 2012.
- [12] R. S. Desikan, F. Ségonne, B. Fischl, B. T. Quinn, B. C. Dickerson, D. Blacker, R. L. Buckner, A. M. Dale, R. P. Maguire, B. T. Hyman *et al.*, "An automated labeling system for subdividing the human cerebral cortex on MRI scans into gyral based regions of interest," *Neuroimage*, vol. 31, no. 3, pp. 968–980, 2006.
- [13] M. Jenkinson, C. F. Beckmann, T. E. Behrens, M. W. Woolrich, and S. M. Smith, "Fsl," *Neuroimage*, vol. 62, no. 2, pp. 782–790, 2012.
- [14] F.-C. Yeh, T. D. Verstynen, Y. Wang, J. C. Fernández-Miranda, and W.-Y. I. Tseng, "Deterministic diffusion fiber tracking improved by quantitative anisotropy," *PLoS one*, vol. 8, no. 11, p. e80713, 2013.
- [15] F.-C. Yeh, V. J. Wedeen, and W.-Y. I. Tseng, "Generalized q-Sampling Imaging," *IEEE Transactions on Medical Imaging*, vol. 29, no. 9, pp. 1626–1635, 2010.
- [16] J. C. Morris, "The clinical dementia rating (cdr): Current version and," *Young*, vol. 41, pp. 1588–1592, 1991.
- [17] V. C. Pangman, J. Sloan, and L. Guse, "An examination of psychometric properties of the mini-mental state examination and the standardized mini-mental state examination: implications for clinical practice," *Applied Nursing Research*, vol. 13, no. 4, pp. 209–213, 2000.